ICAS 2020 SHANG HAI
International Council of the Aeronautical Sciences
32nd Congress of the International Council of the Aeronautical Sciences
September 6-10, 2021
Pudong Shangri-La, Shanghai, China

An Integrated Aerodynamic/Thermal/Structural Design Framework for Hypersonic Vehicles

Li Chang[1], Wan Zhiqiang[1], Wang Xiaozhe[2]

[1] School of Aeronautic Science and Engineering, Beihang University
[2] Institute of Unmanned System, Beihang University

Abstract

Hypersonic vehicle is playing a more and more important role in military and other high-technology fields. However, traditional serial design procedure is inefficient and is not adequate for hypersonic vehicles. This paper proposes an integrated aerodynamic/thermal/structural design framework for hypersonic vehicles. It takes aerodynamic force, aerodynamic heating, heat transfer and structure deformation into account together, which can achieve a more realistic design during the conceptual or preliminary design phase. An integrated aerodynamic/thermal/structure analysis method is developed, in which the piston theory, reference temperature method and finite element method (FEM) are applied for the calculation of aerodynamic force, aerodynamic heating, heat transfer and structure static analysis. The parametric modeling is used to modify the shape and structure size conveniently and consistently. Then the integrated optimization for aerodynamic shape parameters and structure sizes of the model in strictest results of aerothermoelastic analysis is performed to obtain the optimal design parameters. Genetic algorithm is used for the optimization for this integrated optimization. An invalid initial solution turned into a valid solution through the integrated optimization framework proposed in this paper. Besides, a better result evaluated by the combination of structure weight and lift-drag ratio was achieved by the integrated optimization framework for this model by 2.31%.

Keywords: Aeroelasticity, Optimization, Hypersonic vehicles, Flight load, Multidisciplinary optimization

1. Introduction

Hypersonic vehicle has been one of the most popular fields in aeronautics and astronautics research because it has many unique advantages, including high speed which can reach over 5.0 Mach Number and wide flight range [1]. A number of hypersonic vehicles have been or are being devised in recent years, such as X-43A, X-51A and SR-72. However, there are considerable tough problems for hypersonic vehicles, such as unsteady aerodynamic computation methods, effective aeroelastic analysis under the heating environment, panel flutter and complicated coupling of heat, aerodynamic, structure, thrust and other fields [2-3]. Among these problems, severe heating environment and coupling for different kinds of physics fields, including structure, aerodynamics and heating is one of the most basic and typical problem for hypersonic vehicles. When hypersonic vehicles fly in hypersonic flow, intense aerodynamic heating will appear caused by friction between the surface of vehicles and flow, which makes the temperature of the surface improve a lot. It will have a great influence on structure by thermal stress and material property change in structure. Therefore, it is really important to take aerodynamics, structure and heat into account together to get a more realistic flight load condition.

There are many researches on the optimization for hypersonic vehicles. Eyi provided an aerodynamic shape optimization that combined with a high fidelity hypersonic CFD code, LeMANs and Bezier and NURBS modeling methods on IRV-2 [4]. Li utilized the concept of aeroelastic tailing for a structure optimization and a flutter mass balancing optimization for X-56A [5]. FUJIKAWA performed a multidisciplinary optimization considering vehicle geometry, mass property, aerodynamics, propulsion and trajectory for a reusable two-stage-to-orbit launch vehicle [6]. Du developed a robust structure optimization for a hypersonic wing considering the heating uncertainty [7].

Because of the different objectives of structure design and aerodynamic design, if structure and

aerodynamic shape are designed individually, the optimum result will probably not be achieved. Multidisciplinary Analysis and Optimization (MDAO) can offer a solution to balance the different needs of different disciplines. Multidisciplinary optimization has been widely used in engineering, such as aircraft wing design, complete aircraft, spacecraft and other engineering system [8].

However, there were few researches on multidisciplinary optimization on hypersonic vehicles especially considering structure optimization. The complicated coupling of different disciplines is significant especially in hypersonic vehicles. The influence of one discipline on another cannot be omitted when performing one individual analysis for each discipline. If designing different disciplines individually, results will have an obvious deviation from the actual condition. In order to get a more realistic analysis result and a better design, this paper constructs an effective integrated aerodynamic/thermal/structural design framework for hypersonic vehicles. It can produce an optimum design considering aerodynamics, structure and heat during the conceptual or preliminary design phase, which is useful to get a suitable design and reduce the time of redesigning in the following design phases.

First, this paper introduces the methods used for aerodynamic analysis and aerodynamic heating analysis. In order to express the relationship between the aerodynamic shape and geometry parameters, a parameterization method was proposed. Based on these methods, an integrated design framework was proposed to make optimization of aerodynamic and structure design variables for a combined objective with weight and lift-drag ratio. Then, the typical wing of hypersonic vehicle chosen as the example and optimization model will be described in detail. At last, simulation results of the initial model and different optimization approaches will be displayed and compared.

2. Methodology

Because of coupling of different subjects in hypersonic vehicles, different analysis methods of individual disciplines are adapted in this design framework. In aerodynamic analysis, shock-expansion theory and local piston theory are used to acquire the aerodynamic pressure. In aerodynamic heating analysis, Eckert's reference temperature method, Reynolds analogy method and Stefan-Boltzmann thermal radiation law are used to acquire the friction and heat flux. In heat conduction and static structural analysis, FEM is used to get the relatively precise results. In order to describe and modify the shape of the wing precisely and quickly, this paper propose a parameterization method. Furthermore, the integrated aerodynamic/thermal/structural design framework is proposed for the integrated aerodynamic/structural optimization.

2.1 Aerodynamic Analysis Method

There are several commonly used engineering methods to compute the aerodynamic forces in hypersonic vehicles, such as piston theory, Van Dyke theory and Newton impact theory [2]. Among them, piston theory proposed by Lighthill is used most frequently for hypersonic wings with thin airfoil. Local piston theory is a method improved from the piston theory by using local air parameters to compute the pressure more precisely.

Shock/expansion theory is an analytical method in 2D when the hypersonic airflow flows through the wedge. It computes the air parameter ratios before and after oblique shock wave or expansion wave after computing the relationship between oblique shock angle and wedge angle, which is shown in Equation (1).

$$\tan\theta = 2\cot\beta \frac{Ma_\infty^2 \sin^2\beta - 1}{Ma_\infty^2\left(\gamma + \cos 2\beta\right) + 2} \tag{1}$$

Local piston theory is a commonly used method for hypersonic flow in engineering. It draws an analogy between the disturbed stream field and piston to get the aerodynamic pressure coefficient, which is shown in Equation (2).

$$C_p(x,t) = \frac{2}{Ma_{local}{}^2}\left[\frac{v_n}{a_{local}} + \frac{\gamma+1}{4}\left(\frac{v_n}{a_{local}}\right)^2 + \frac{\gamma+1}{12}\left(\frac{v_n}{a_{local}}\right)^3\right] \tag{2}$$

In order to evaluate the lift-drag ratio of the wing, the drag is calculated by the integral of pressure and friction of all the aerodynamic elements along the flow direction. The lift can also be calculated by the integral of pressure vertical to the flow direction.

2.2 Aerodynamic Heating Analysis Method

This paper uses Eckert's reference temperature method to compute the local flow parameters near the boundary layer between the surface and compressible flow by assuming a reference temperature in incompressible flow. By this method, results solved in incompressible flow can be applied for compressible flow. The relationship between the two kinds of temperature is shown in Equation (3).

$$T^* = 0.5T_w + 0.22T_r + 0.28T_e \tag{3}$$

Based on the Blasius solution, we can acquire the friction stress by local flow parameters solved in Equation (3).Got the reference temperature and friction stress, this paper uses Reynolds analogy method to establish the relationship between the convective heat transfer coefficient and friction stress, which is shown in Equation (4).

$$St^* = \frac{C_f^*}{2\,\mathrm{Pr}^{\frac{2}{3}}} \tag{4}$$

Based on Equation (4), the heat flux caused by the convection and radiation can be calculated from Equation (5) and (6).

$$Q_{conv} = \rho u C_p \left(T_r - T_w\right) St^* \tag{5}$$

$$Q_{rad} = \sigma\varepsilon\left(T_w^4 - T_\infty^4\right) \tag{6}$$

2.3 Parameterization of Shape and Structure

In order to change grid coordinates of finite element model conveniently and precisely, this article proposed a parameterization approach to this hypersonic wing considering changes of the length of the wing span, L, the swept angle of the leading edge, χ and the root-tip ratio, η. The root-tip ratio η can be expressed as the ratio of the length of the wing root chord, C_0 and the length of the wing tip chord, C_1. The variables with superscript '0' are the variables of the initial model while the variables with subscripts mean the location in span direction. The leading point coordinates of the wing root $\left(x_0, y_0, z_0\right)$ is assumed to $\left(0,0,0\right)$, which can simplify the equations below a lot. We can express the shadow area of the wing, S by L, χ and η, the relations of which are listed in Equation (7).

$$S = \left(C_0 + C_1\right)L = C_0\left(1+\frac{1}{\eta}\right)L \tag{7}$$

In order to guarantee the shadow area of the wing, S a constant, that means the area of the new model, S must be equal to the area of the initial model, S^0, as shown in Equation (8).

$$S = C_0\left(1+\frac{1}{\eta}\right)L = S^0 = C_0^0\left(1+\frac{1}{\eta^0}\right)L^0 \tag{8}$$

From Equation (8), we can deduce the relationship between the length of the wing root chord, C_0 and the length of the initial wing root chord, C_0^0, as shown in Equation (9).

$$\frac{C_0}{C_0^0} = \frac{\left(1+\frac{1}{\eta^0}\right)L^0}{\left(1+\frac{1}{\eta}\right)L} \tag{9}$$

At first, we can deduce the coordinates of the leading grid, as shown in Equation (10).

$$\left(x_l, y_l, z_l\right) = \left(x_0 + y^0\frac{L}{L^0}\tan\chi, y^0\frac{L}{L^0}, z^0\right) \tag{10}$$

Besides, we can deduce the length of the local chord at y^0 coordinate of the initial model and the modified model, as shown in Equation (11) and (12).

$$C_y^0 = \left[\frac{\left(\frac{1}{\eta^0} - 1 \right)}{L^0} y^0 + 1 \right] C_0^0 \tag{11}$$

$$C_y = \left[\frac{\left(\frac{1}{\eta} - 1 \right)}{L^0} y + 1 \right] C_0 \tag{12}$$

And then, we can deduce the relative location in chord direction between the distance of the grid and local leading point contrast with the length of the local chord, as shown in Equation (13).

$$\frac{x^0 - \left(x_0 + y^0 \tan \chi^0 \right)}{C_0^0} \tag{13}$$

Because of the same coordinate proportion in chord direction in the initial model and modified model, we can derive the x coordinate of the modified model at y coordinate from the proportion, the length and leading point coordinate of local chord, as shown in Equation (14).

$$x = x_0 + y^0 \frac{L}{L^0} \tan \chi + \left[x^0 - \left(x_0 + y^0 \tan \chi^0 \right) \right] \frac{\frac{\left(\frac{1}{\eta} - 1 \right)}{L^0} y + 1}{\frac{\left(\frac{1}{\eta^0} - 1 \right)}{L^0} y^0 + 1} \frac{\left(1 + \frac{1}{\eta^0} \right) L^0}{\left(1 + \frac{1}{\eta} \right) L} \tag{14}$$

Besides, the relationship of the y and z coordinates between the initial and modified model can be described as Equation (15) and (16).

$$y = y^0 \frac{L}{L^0} \tag{15}$$

$$z = z^0 \tag{16}$$

Given the leading point coordinates of the wing root (x_0, y_0, z_0) and the initial grid coordinates (x^0, y^0, z^0), we can obtain the transformed coordinates (x, y, z), as shown in Equation (14), (15) and (16).

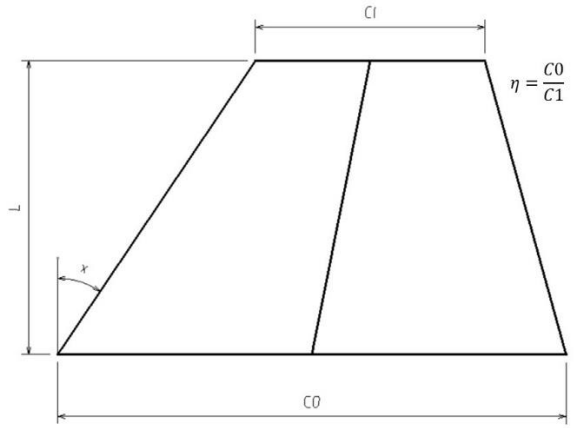

Figure 1 - The sketch of design variable of the aerodynamic shape

2.4 Integrated Design Framework

An integrated aerodynamic/thermal/structural design framework shown in Figure 2 is proposed for hypersonic vehicles. The design procedure is carried out from top to bottom. The steps on the left

side are mainly relevant to aerodynamics, ones on the right side are mainly about heat, while the middle ones are the main parts of the procedure, which are primarily concerned with structure.

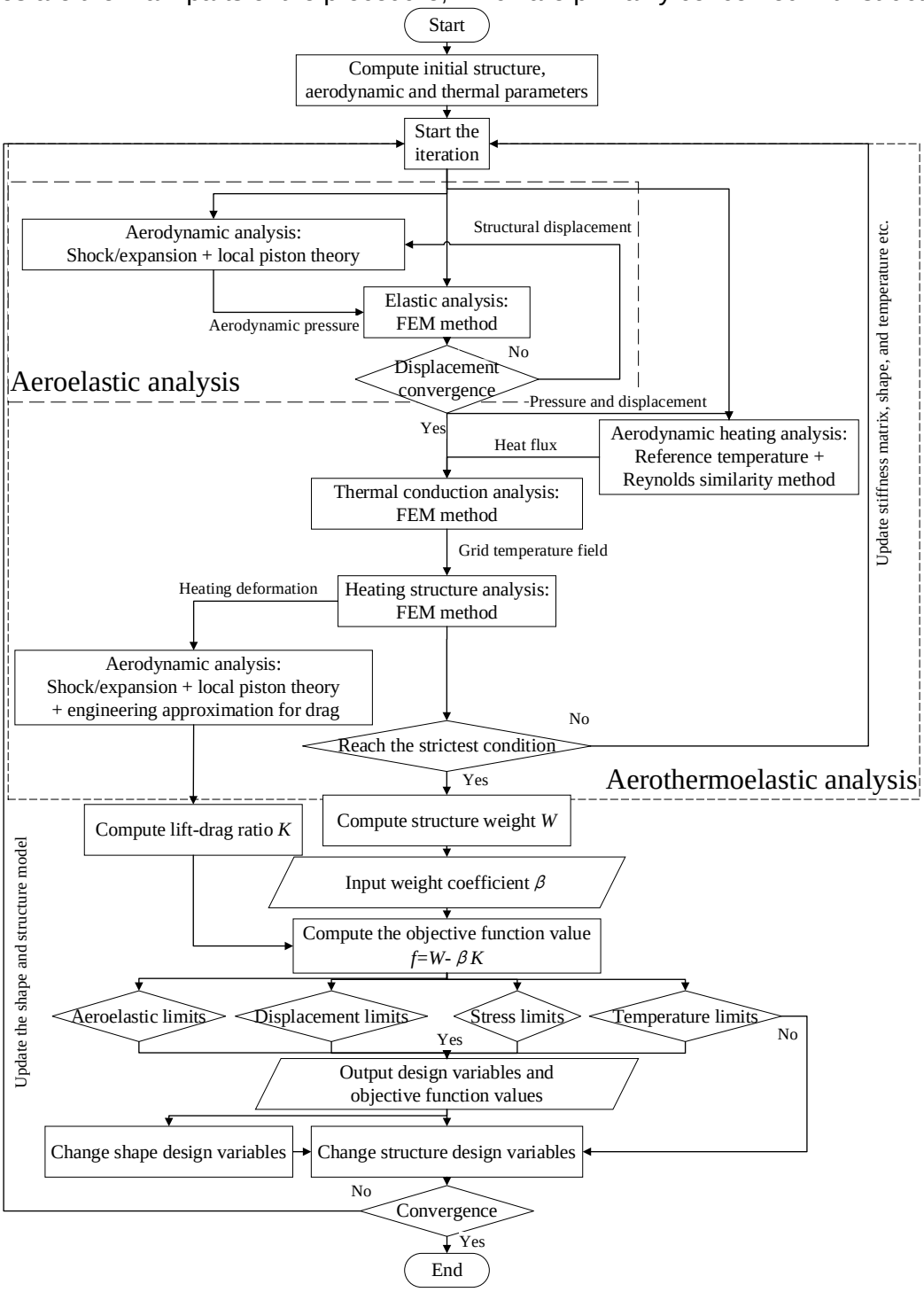

Figure 2 - Flowchart of aerodynamic/thermal/structural integrated design framework

The design progress and detailed steps are as follows:

1) Compute the initial structural, flow and temperature parameters.
2) Get into the iteration of Aerothermoelasticity.
3) Perform aerodynamic analysis. In order to compute the aerodynamic forces in hypersonic flow rapidly, this paper adapts shock/expansion theory to compute the local flow parameter and local piston theory to compute aerodynamic pressure on the surface.
4) Perform static analysis on which aerodynamic forces are applied by Finite Element Method (FEM).
5) Repeat 3) and 4), at the same time, interpolate structure grid displacements to the aerodynamic shape grids and aerodynamic forces to the structure until the displacement comes to convergence. That is the aeroelastic analysis.

6) Perform aerodynamic heating analysis. This paper uses Eckert's reference temperature method and Reynolds analogy method to compute the heat flux caused by convection and Stefan-Boltzmann thermal radiation law to compute the heat flux caused by radiation.
7) Perform thermal conduction analysis to compute the temperature field of structure caused by the heat flux on the surface by FEM.
8) Perform heating structure analysis by FEM.
9) Judge whether the strictest condition is reached. If yes, go to the next step after completing the Aerothermoelastic analysis. Otherwise, go back to 2) to make the Aerothermoelastic analysis for the next time step.
   According the previous research for Aerothermoelastic analysis for hypersonic vehicles by Du in [7], in chronological order, the maximum thermal deformation will rise significantly in first few seconds, then reach the peak, descend gradually in a long time and finally be stabilized at a certain value.
   The strictest condition is defined as the case when the maximum thermal deformation reach the peak in this paper. Besides, in the first few iterations of aeroelasticity and thermal conduction, it is not be converged to the exact results of those moments and a little fluctuation of thermal deformations probably occur. In order to avoid this situation, the judging criteria is defined as the difference between the thermal deformation of the previous moment and the thermal deformation of the next moment in two consecutive times.
10) Perform aerodynamic analysis by shock/expansion, local piston theory and engineering approximation method for drag.
11) Compute lift-drag ratio K and structure weight W.
12) Input the user-defined weight coefficient β according to actual consideration about aerodynamics and structure.
13) Compute the objective function value $f = W - \beta K$.
14) Evaluate whether or not the result meets the constraints, such as aeroelastic limits, displacement limits, stress limits and temperature limits. If yes, it is proved to be in the feasible region and a valid design point. Retain the result, output the value of design variables and objective function and go to the next step. Otherwise, abandon this point and go to the next step.
15) Change the design variable parameters of aerodynamic shape and structure size.
16) Judge whether the convergence is reached. If yes, it will come to the end and optimization will be completed. Otherwise, update the models of aerodynamic shape and structure by the parameterization method presented in 2.3, go back to 2) and start another iteration.

3. Model Description

3.1 Aerodynamic Shape and Structure Model

This paper uses a typical hypersonic low-aspect-ratio trapezoidal wing for the research. The geometry and the structure model are shown individually in Figure 3 and Figure 4. To protect the structure from severe aerodynamic heating, the whole wing is divided into three parts from outside to inside, including heat shield layer made of Rene, insulation layer made of Min-K and structural skin made of TIMETAL 834. As shown in Figure 3, wing skin is divided into four regions, including front part of the upper surface, back part of the upper surface and the front and back ones of the lower surface. The thickness of these four regions of wing skin are defined as the design variables of the structure respectively called t_1, t_2, t_3, t_4. The initial shape parameters of the model are shown in the Figure 3, including the length of the wing root chord and the wing span and the swept angle of the leading edge and the trailing edge. As shown in Figure 1, three aerodynamic shape parameters are defined as the design variables, including the length of the wing span, L, the swept angle of the leading edge, χ and the root-tip ratio, $\eta = \frac{C_0}{C_1}$, computed from the ratio of the length of wing root chord to the length of wing tip chord.

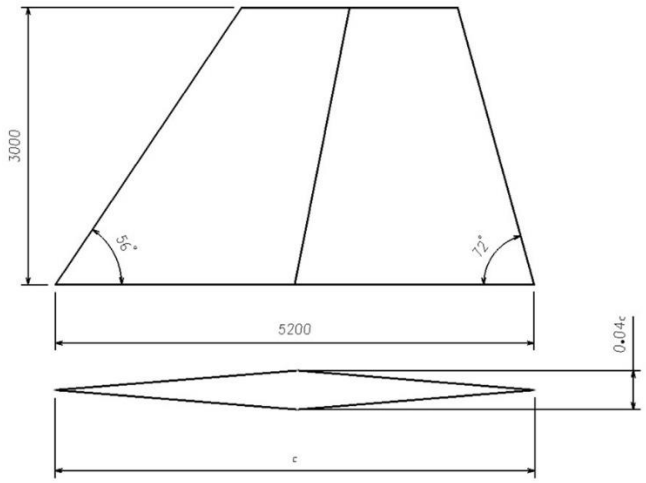

Figure 3 - The initial shape of the model

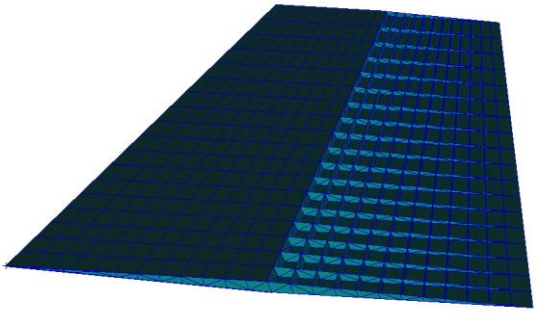

Figure 4 - Finite element model of the wing structure

3.2 Optimization Model

The optimization model is described as below:

Objective: Minimize

$$f = W - \beta K \tag{17}$$

In Equation (17), *f* is the total objective, *W* is the weight of the structure, β is the weighting factor defined by user and *K* is the lift-drag ratio.

Design variables:

$$t_1, t_2, t_3, t_4, L, \eta, \chi$$

The initial values, limits and units of the design variables are shown in Table 1.

Table 1 - List of Design Variables

Name	t_1	t_2	t_3	t_4	L	η	χ
Initial Value	3.0	3.0	3.0	3.0	3.0	2.363636	34.0
Lower Limit	2.5	2.5	2.5	2.5	2.8	2.3	32.0
Upper Limit	3.5	3.5	3.5	3.5	3.2	2.4	36.0
Unit	mm	mm	mm	mm	m	-	degree

Constraint conditions:

1) Stresses in all the structure elements must be less than 760MPa.
2) Strains in all the structure elements must be less than 10^{-4}.
3) The vertical deflection of the wing tip must be less than 110mm.
4) The rotation angle of the wing tip must be less than 4°.

3.3 Flight Conditions

Essential flight condition parameters are defined as follows:

Cruising altitude is 15 kilometers.

Mach number is 8.

Angle of attack is 6 degrees.

Time step for the coupling of aeroelasticity and heat conduction is 4 seconds.

Time step for each heat conduction analysis is 0.1 second.

3.4 Genetic Algorithm parameters

Population size is 30.

Generation number is 5.

Crossover probability is 0.7.

Mutation probability is 0.4.

4. Results

4.1 Analysis for the Initial Model

At first, an aerothermoelastic analysis for the initial model was performed as a reference of other optimum solutions below. Figure 5 shows the variation of maximum deformation over time. In first 40 seconds, the maximum deformation rises vastly; at about 40 seconds, the maximum thermal deformation reaches a peak of 119.5 mm; in the rest of time, the maximum deformation descends gently and finally comes to a steady value. Besides, thermal deformation is much larger than the deformation caused by aeroelasticity only.

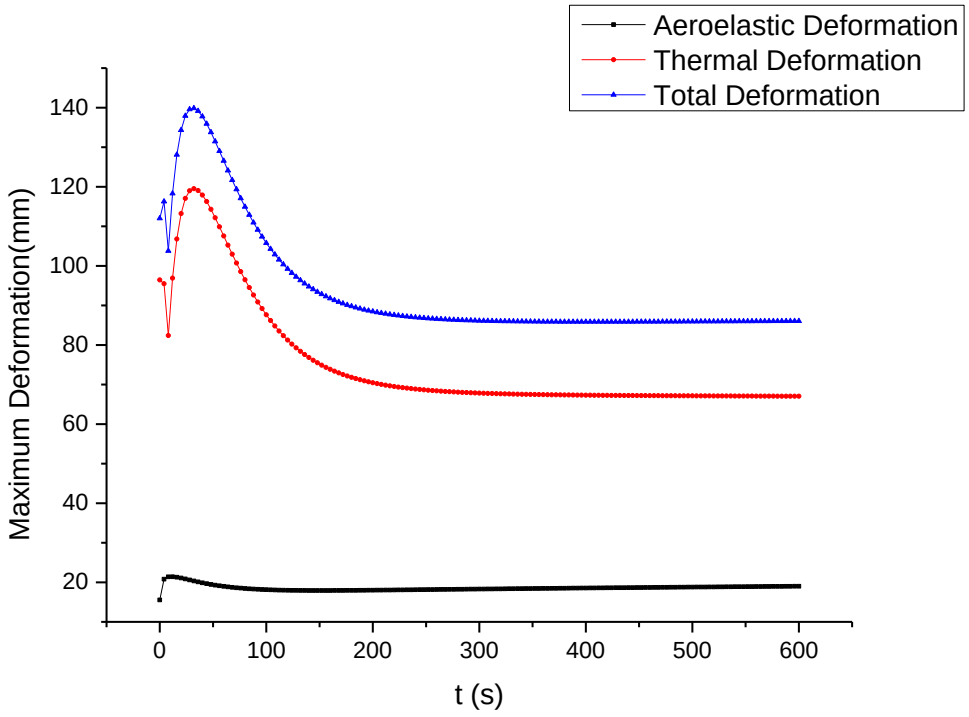

Figure 5 - Maximum deformation of the initial model over time

The objectives and restricts of the initial model are listed in Table 2. The weight of structure is 2295.5kg while the lift-drag ratio is 6.60455 but the maximum stress and the maximum tip vertical deformation exceed the restrictions. Thus, it was not a valid solution and needed to be optimized to get a valid solution. Besides, in order to reveal the variation trend of the load condition with time, the temperature distributions on the upper and lower surface in different moments are displayed in Figure 6, Figure 7, and Figure 8. As we can see, the maximum temperature on the surface in the first iteration is about 1000K. However, when the strictest condition comes at about 40s, the maximum temperature will reach over 2000K, much larger than the one in 4s. The maximum temperature at 600s is a little lower than the strictest condition. In addition, the maximum temperature appears at the leading edge on the lower surface and the area of high temperature spreads with time.

Table 2 - Objectives and restricts of the initial model

Name	Weight	Lift-drag Ratio	Total Objective	Maximum Stress	Maximum Strain	Maximum Tip Displacement	Maximum Tip Rotation Angle
Value	2295.5	6.60455	1635.045	783.87	-1.5953	114.92	0.6227
Unit	kg	-	-	Mpa	$\times 10^{-4}$	mm	°

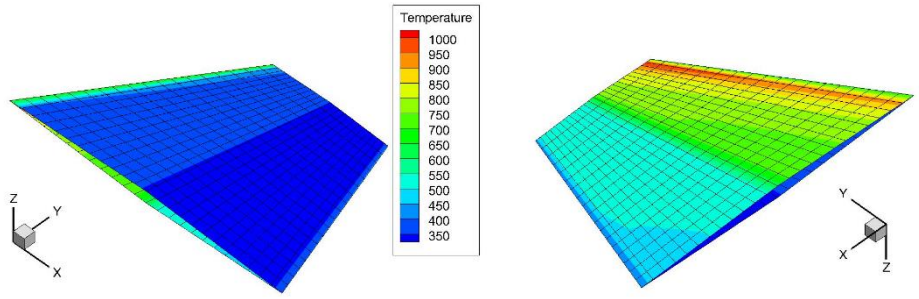

Figure 6 - Temperature distribution on upper and lower surface of the initial model at 4s

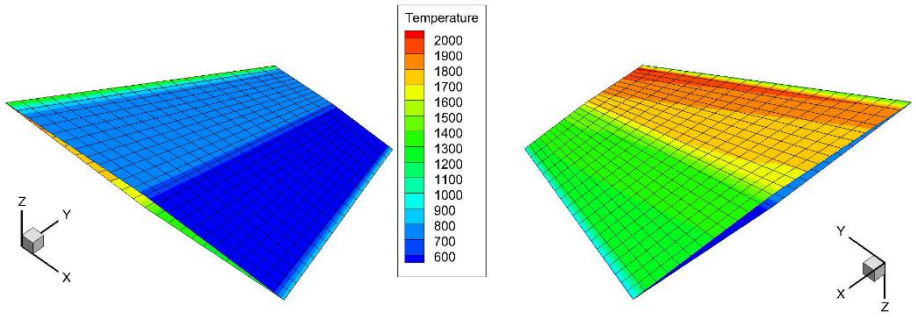

Figure 7 - Temperature distribution on upper and lower surface of the initial model at the strictest condition

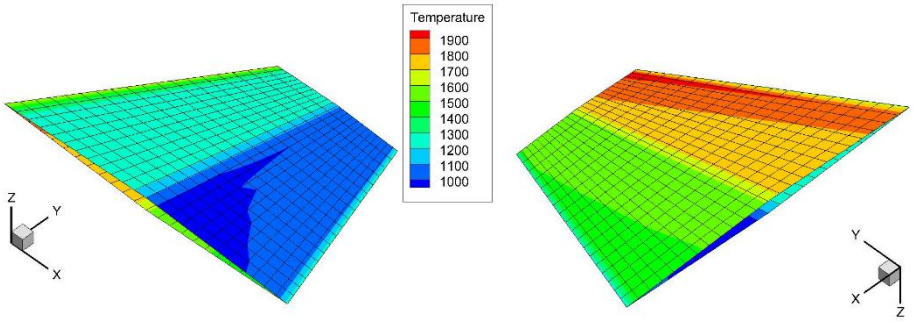

Figure 8 - Temperature distribution on upper and lower surface of the initial model at 600s

4.2 Structural Optimization

If do not consider the effect of aerodynamics, the optimization will be conducted without aerodynamic design variables, aerodynamic objectives and the modifications of shape and grid locations, which can make the optimization procedure more concise and easier to perform. The 10), 11), 12), 13), 16) steps in the integrated optimization framework described in Section 2.4 can be removed or simplified with aerodynamic variables. The results and values of optimal solution by structural optimization are displayed in Table 3 and Table 4.

Table 3 - Design variables of the optimal solution by structural optimization

Name	t_1	t_2	t_3	t_4
Value	2.58	2.66	3.44	3.36
Unit	mm	mm	mm	mm

Table 4 - Objectives and restricts of the optimal solution by structural optimization

Name	Weight	Lift-drag Ratio	Total Objective	Maximum Stress	Maximum Strain	Maximum Tip Displacement	Maximum Tip Rotation Angle
Value	2296.5	6.62136	1634.364	758.80	-1.5592	115.01	0.5537
Unit	kg	-	-	Mpa	$\times 10^{-4}$	mm	°

As shown in Table 4, the optimal solution by the traditional structure optimization is a little improved. Both the maximum stress and the maximum tip displacement are decreased but the maximum tip displacement is still out of the restriction. The structure weight is heavier than the initial model but the total objective is improved slightly.

4.3 Complete Integrated Optimization

In this section, results of the optimal solution by the integrated optimization framework proposed in Section 2.4 are displayed. The weighting factor β is defined as 100.0 here considering the values of the weight W and the lift-drag ratio K in the previous solution in Section 4.1 and 4.2. The design variables, objectives and restricts of the optimal solution by integrated optimization are listed in Table 5 and Table 6. It can be seen that all the restricts are satisfied. Besides, the structure weight, lift-drag ratio and total objective are all improved by the integrated optimization compared to the initial model by 1.09%, 1.91% and 2.31%. In addition, the results are also improved compared to the optimal solution by the traditional structural optimization.

Table 5 - Design variables of the optimal solution by integrated optimization

Name	t_1	t_2	t_3	t_4	L	η	χ
Value	2.65	2.66	2.52	3.22	2.972	2.383	35.88
Unit	mm	mm	mm	mm	m	-	degree

Table 6 - Objectives and restricts of the optimal solution by integrated optimization

Name	Weight	Lift-drag Ratio	Total Objective	Maximum Stress	Maximum Strain	Maximum Tip Displacement	Maximum Tip Rotation Angle
Value	2270.4	6.73076	1597.324	750.95	-1.7744	109.85	0.5987
Unit	kg	-	-	Mpa	$\times 10^{-4}$	mm	°

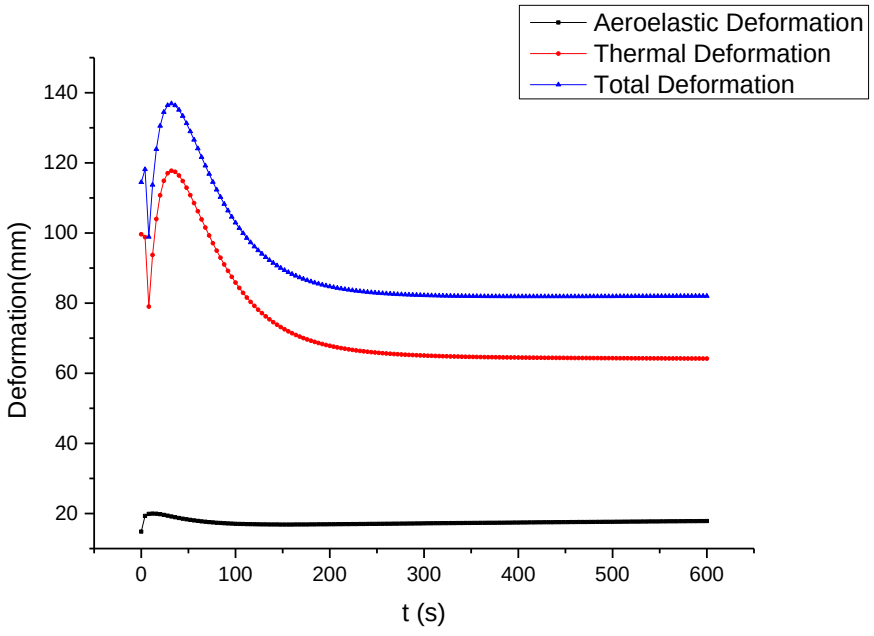

Figure 9 - Maximum deformation of optimal solution by integrated optimization over time

Besides, the maximum deformations change with time are displayed in Figure 9. As we can see the trend of the maximum deformations is nearly the same as the one of the initial model, which can prove the judgement of the strictest condition to be correct.

5. Conclusion

Hypersonic vehicle has been a focus of aeronautics and astronautics research because of its military application value and severe challenges, which is different from traditional aircraft design. In order to give full consideration to the complicated coupling of various subjects better, this paper proposes an aerodynamic/thermal/structural integrated optimization framework which can take structure and aerodynamic design variables and objectives into account together. Both traditional structure optimization and integrated optimization were performed for the strictest condition of a typical low-aspect-ratio trapezoidal hypersonic wing in this paper. An apparent improvement in the comprehensive performance combined with structure objective evaluated by the weight and aerodynamic object evaluated by the lift-drag ratio appeared in the optimization for the example wing. Thus, the aerodynamic/thermal/structural integrated optimization framework proposed in this paper is proved to be effective and efficient for hypersonic vehicles and it is worth considering to perform an integrated optimization in the preliminary design for hypersonic vehicles.

References

[1] Cui Erjie, Research statutes, development trends and key technical problems of near space flying vehicles (in Chinese). *Chinese Advances in Mechanics*, Vol.39, No.6, pp 658-673, 2001.

[2] Yang Chao, Review of studies on aeroelasticity of hypersonic vehicles (in Chinese), *Chinese Journal of Aeronautics*, Vol.31, No.1, pp. 1-11, 2010.

[3] Yang Chao, Research progress of aerothermoelasticity of air-breathing hypersonic vehicles (in Chinese), *Journal of Beijing University of Aeronautics and Astronautics*, Vol.45 No.10, pp. 1911-1923, 2019.

[4] Sinan Eyi, Aerothermodynamic design optimization of hypersonic vehicles, *Journal of Thermophysics and Heat Transfer*, Vol. 33, No. 2, 2019.

[5] Wesley W. Li, Aeroelastic optimization study based on the X-56A model, *AIAA Atmospheric Flight Mechanics Conference*, Atlanta, GA, 2014.

[6] Takahiro FUJIKAWA, Multidisciplinary Design Optimization of a Two-Stage-to-Orbit Reusable Launch Vehicle with Ethanol-Fueled Rocket-Based Combined Cycle Engines, *Trans. Japan Soc. Aero. Space Sci*. Japan, Vol. 60, No. 5, pp. 255–265, 2017.

[7] Du Ziliang, Robust Aeroelastic Design Optimization of Hypersonic Wings Considering Uncertainty in Heat Flux, *Trans. Japan Soc. Aero. Space Sci*. Japan, Vol. 60, No. 3, pp. 152–163, 2017.

[8] Joaquim R. R. A. Martins, Multidisciplinary Design Optimization: A Survey of Architectures, AIAA Journal, vol.51, No.9, pp 2049-2075, 2013.

Copyright Statement